Electronic Supplementary Information (ESI)

Imidazole additives in 2D halide perovskites: Impacts of –CN versus –CH_3 substituents reveal the mediation of crystal growth by phase buffering

Shuang Yu,[a] *Jie Meng,*[b] *Qinying Pan,*[d] *Qian Zhao,*[b] *Tõnu Pullerits,*[d] *Yingguo Yang,*[*c]
Kaibo Zheng[*b] *and Ziqi Liang*[*a]

[*][a]Prof. Z. Liang, S. Yu
Department of Materials Science
Fudan University
Shanghai 200433, China
Email: zqliang@fudan.edu.cn

[*][b]Dr. K. Zheng, J. Meng, Qian Zhao
Department of Chemistry
Technical University of Denmark
DK-2800 Kongens Lyngby, Denmark
Email: kzheng@kemi.dtu.dk

[*][c]Dr. Y. Yang
Shanghai Synchrotron Radiation Facility (SSRF)
Shanghai Advanced Research Institute & Chinese Academy of Sciences
Shanghai 201204, China
Email: yangyingguo@sinap.ac.cn

[d]Dr. Q. Pan, Prof. T. Pullerits
Department of Chemical Physics and NanoLund
Lund University
Box 124, 22100 Lund, Sweden

Experimental Section

Materials: PbI_2 and CH_3NH_3I were purchased from Maituowei Ltd. (China). phenethylamine was purchased from Energy Chemical. All other chemicals were purchased from J&K Scientific, Ltd. (China). All the reagents were used as received.

Fabrication of 2D RPP Thin Films: The $PEA_2MA_3Pb_4I_{13}$ precursor solutions (40 wt%) prepared by mixing PbI_2, HI, CH_3NH_3I and PEA at corresponding stoichiometric ratios in mixed solvent of DMF and DMSO (100:3 vol%). The DMI and DCI additive are dissolved into DMF (20 mg/1 ml), which was added into above 2D RPP precursor (50 μl/1 ml) after adequate dissolution. All the 2D RPP films were obtained by spin-coating the precursor solutions at 5000 rpm for 60 s at room temperature. Toluene was dripped on the spinning wet 2D RPP at 5 second. Part of the samples was treated by thermal annealing at 100 °C for 10 min.

Characterization: Optical absorption spectra of samples were acquired on Agilent 8453 UV-Visible spectrophotometer. Steady-state photoluminescence was measured using a FluoroMax$^{@}$-4 spectrofluorometer (HORIBA JOBIN YVON, Inc., Edison, NJ) with the excitation beam at 500 nm. The PL intensity was then corrected by absorbed photon numbers at the exciting light wavelength. X-ray diffraction pattern data for 2θ values were collected with a Bruker AX D8 Advance diffractometer with nickel filtered Cu Kα radiation ($\lambda = 1.5406$ Å). Field-emission scanning electron microscopy images coupled with energy-dispersive X-ray elemental analysis were acquired on Philips XL-30 field-emission gun at an accelerating voltage of up to 30 kV. Transient absorption spectrsocopy (TAS) experiments were performed by using a femtosecond pump-probe setup in nitrogen atmosphere. Laser pulses (800 nm, 80 fs pulse length, 1 kHz repetition rate) were generated by a regenerative amplifier (Spitfire XP Pro) seeded by a femtosecond oscillator (Mai Tai SP, both Spectra Physics). The pump pulses at 400 nm were generated by a BBO crystal as a second harmonic of the laser. The used excitation photon fluxes are 3×10^{12} and 1.5×10^{14} photons/cm^2/pulse. For the probe, we used the super-continuum generation from a thin CaF_2 plate. The mutual polarization between pump and probe beams was set to the magic angle (54.7°) by placing a Berek compensator in the pump beam. The probe pulse and the reference pulse were dispersed in a spectrograph and detected by a diode array (Pascher Instruments). In order to avoid photo-damage, the sample was moved to a fresh spot after each time delay point. Global SVD analysis was performed with the Glotaran software package (http://glotaran.org). These methods yield more accurate fits of rate constants because they treat the full data set as a whole. A simple sequential decay model with various components is chosen for every fitting. Time-resolved photoluminescence (TRPL) spectra were obtained using a streak camera (Hamamatsu, C6860). The laser source is an amplified titanium/sapphire laser providing 800 nm 35-fs pulses at 2 kHz which is then frequency doubled for 400 nm excitation. The B3LYP density functional method with the D3(BJ) dispersion correction was employed in this work to carry out all the computations. The 6-31+G(d,p) basis set was used for C, H, N atoms and SDD basis set for Pb and I atoms. Optimized geometries were verified as minima (zero imaginary frequencies) by frequency calculations at the same level of theory.

Device Fabrication and Measurements: ITO substrates were cleaned sequentially in an ultrasonic bath with deionized water, acetone, and isopropyl alcohol for 20 min, respectively, and then dried under nitrogen. The substrates were oxidized in UV-ozone for 20 min before use. The PEDOT:PSS layers were spin-coated on the patterned substrates at 3000 rpm for 60 s and annealed at 130 °C for 30 min. The substrates coated PEDOT:PSS were transferred to a N_2 filled glovebox for making the active layers. After the formation of the perovskite layer, a solution of PCBM (20mg/ml in chlorobenzene) and BCP (saturated solution in IPA) were spin-coated at 3000 rpm for 50 s 6000 rpm for 30s, respectively. Finally, Ag electrode of 1200 nm were thermally deposited with a rate of 0.5 Å/s for 200 nm and then 1.8 Å/s for 1000 nm, respectively. The active area as defined shadow mask is ~0.04 cm^2. The sample was mounted inside a nitrogen-filled sample holder with a quartz optical window for subsequent measurements. The device reproducibility is improved by strictly maintaining the moisture/oxygen ratio and temperature in the inert atmosphere glovebox. The light *J–V* curves were measured on a Keithley 2400 source meter unit under AM 1.5G light illumination with a Newport-Oriel (Sol3A Class AAA Solar Simulator, 94043A) solar simulator operating at an intensity of 100 mW cm^{-2}. The light intensity was calibrated by a certified Oriel reference cell (91150V) and verified with a NREL calibrated, filtered Si diode (Hamamatsu, S1787-04). The *J–V* profiles were obtained under both forward (−0.5 V

→ +1.5 V) and reverse (+1.5 V → −0.5 V) scans. External quantum efficiency (EQE) spectra were measured on a commercial EQE set-up (QE-R, Enli Technology Co., Ltd). A calibrated silicon diode with a known spectral response was used as a reference.

Results

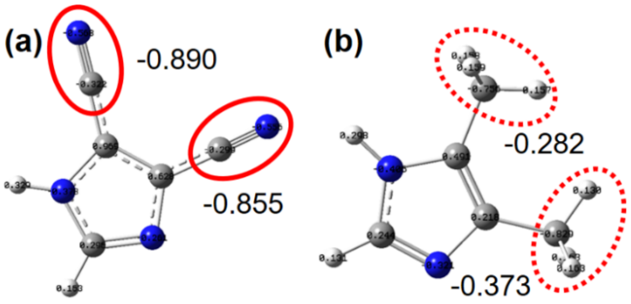

Fig. S1 Atomic electronegativity distribution in (a) DCI and (b) DMI additives.

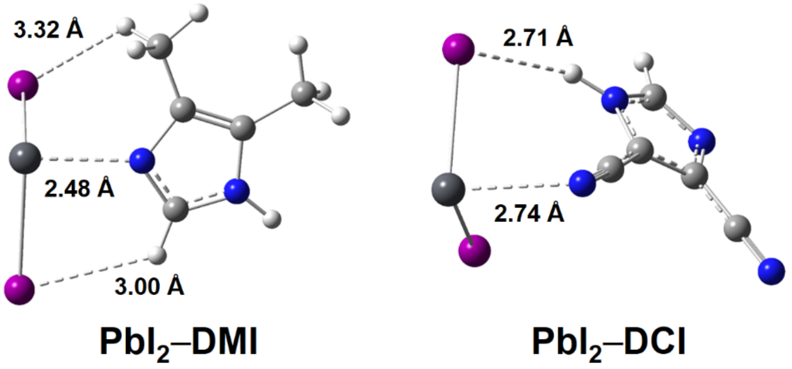

Fig. S2 First-principle calculation of molecular configuration and interaction distance between PbI_2 molecule and DMI/DCI additive.

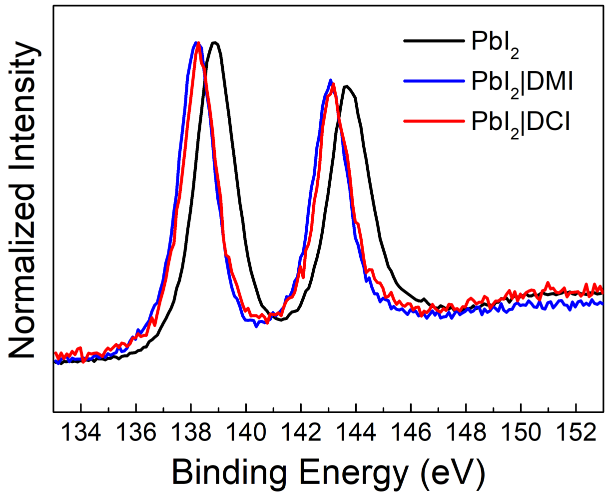

Fig. S3 XPS spectra of neat and additive-treated PbI$_2$ films.

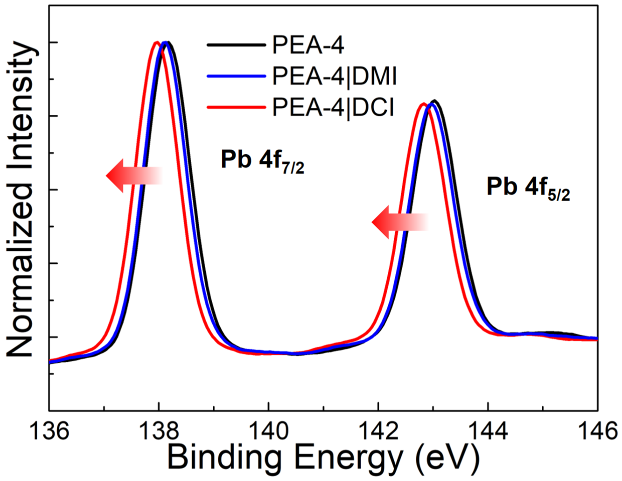

Fig. S4 XPS spectra of neat and additive-treated 2D PEA-4 perovskites.

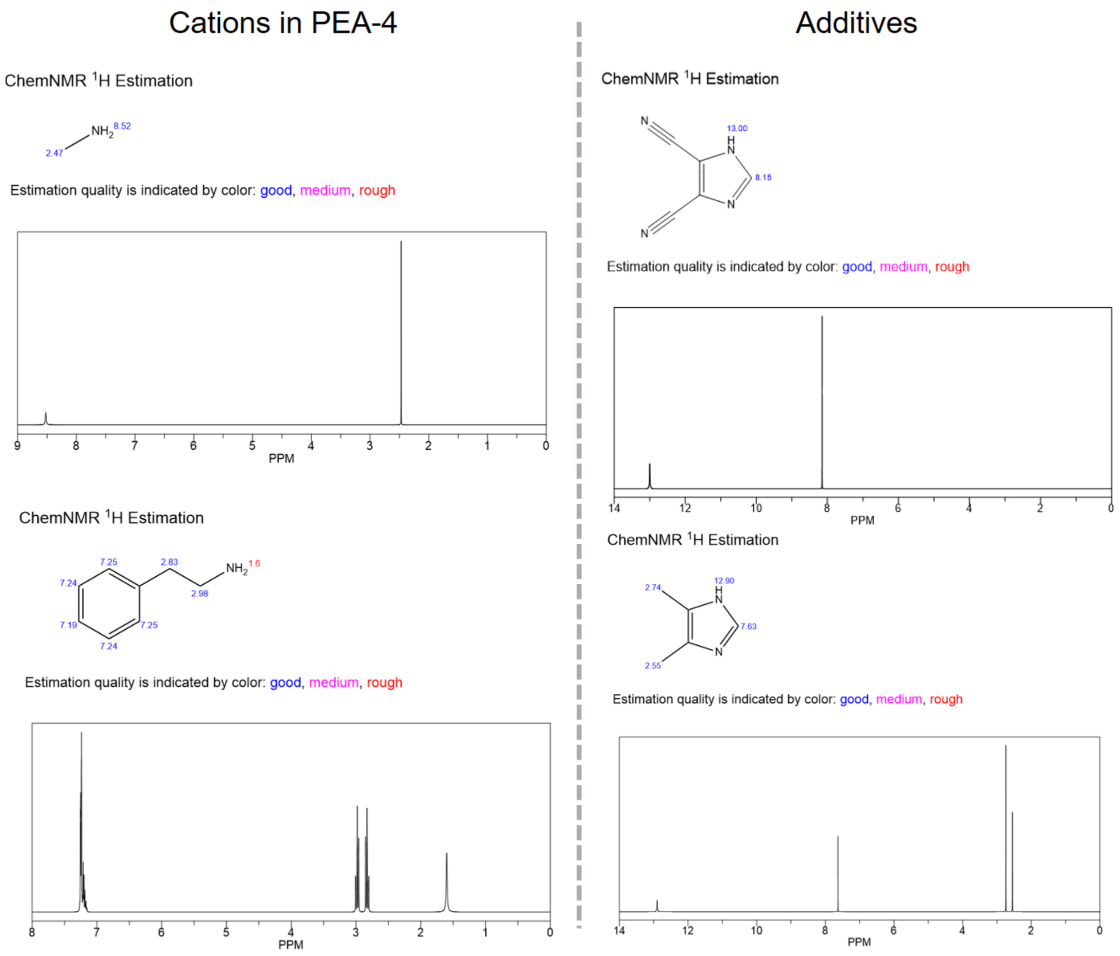

Fig. S5 Predicted ^{1}H-NMR spectra via ChemDraw Professional software.

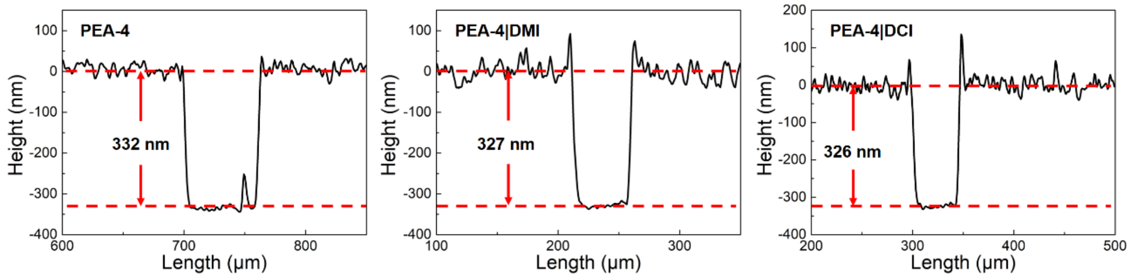

Fig. S6 Layer thickness of neat and additive-treated PEA-4 2D perovskite films determined by step profiler.

Table S1. XRD parameters of 2D pristine PEA-4 as well as DMI and DCI treated PEA-4 perovskites

Sample	2-Theta	d(A)	FWHM
PEA-4	14.00	6.32	0.24
	28.42	3.14	0.39
PEA-4|DMI	13.99	6.33	0.24
	28.40	3.14	0.47
PEA-4|DCI	14.03	6.31	0.31
	28.42	3.14	0.47

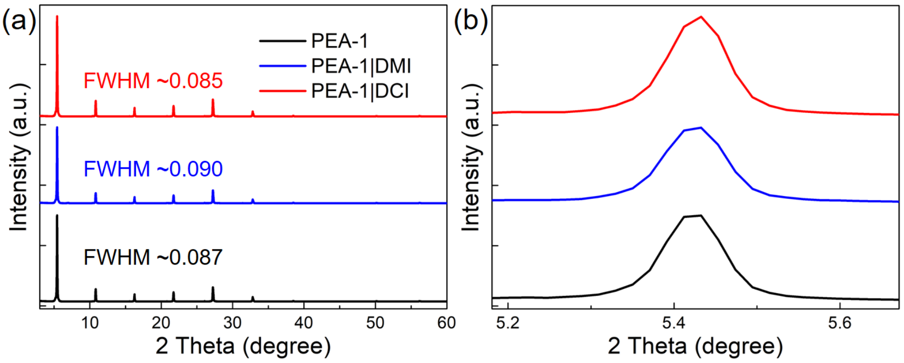

Fig. S7 (a) XRD patterns of pristine PEA-1, DMI and DCI treated PEA-1 films. (b) The enlarged diffraction peaks around 5°.

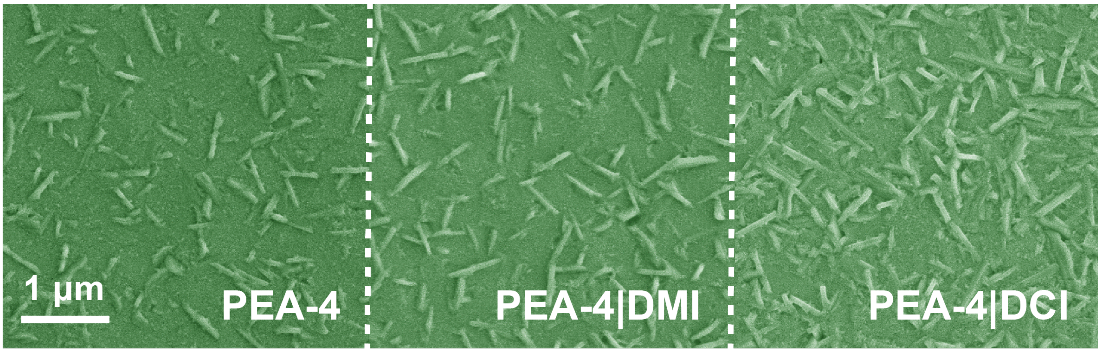

Fig. S8 Top-view SEM images of pristine PEA-4, DMI and DCI treated PEA-4 films.

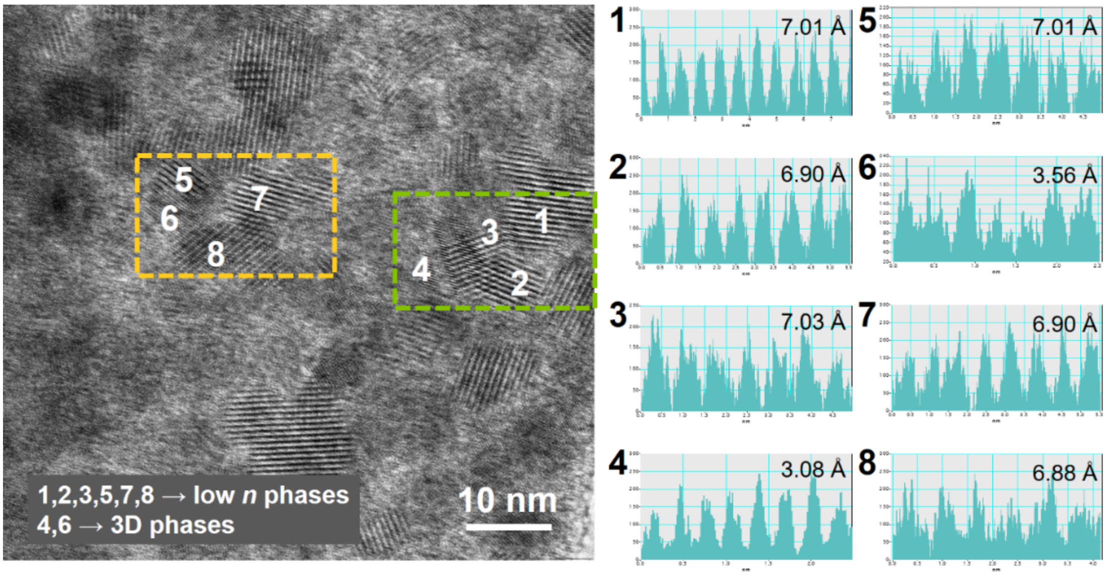

Fig. S9 HR-TEM image of DCI-treated PEA-4 and the corresponding lattice spacings of each phase as labeled.

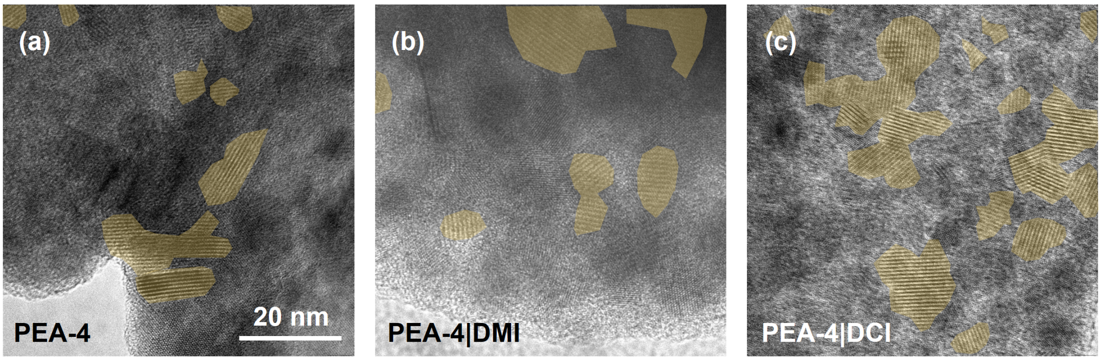

Fig. S10 HR-TEM images of (a) PEA-1, (b) DMI- and (c) DCI-treated PEA-1 films. The highlighted yellow regions refer to 2D phases.

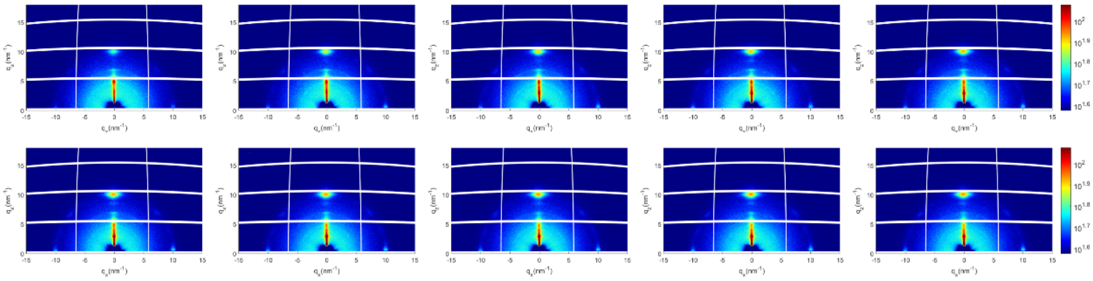

Fig. S11 2D GIWAXS patterns of phase buffering during crystal growth process.

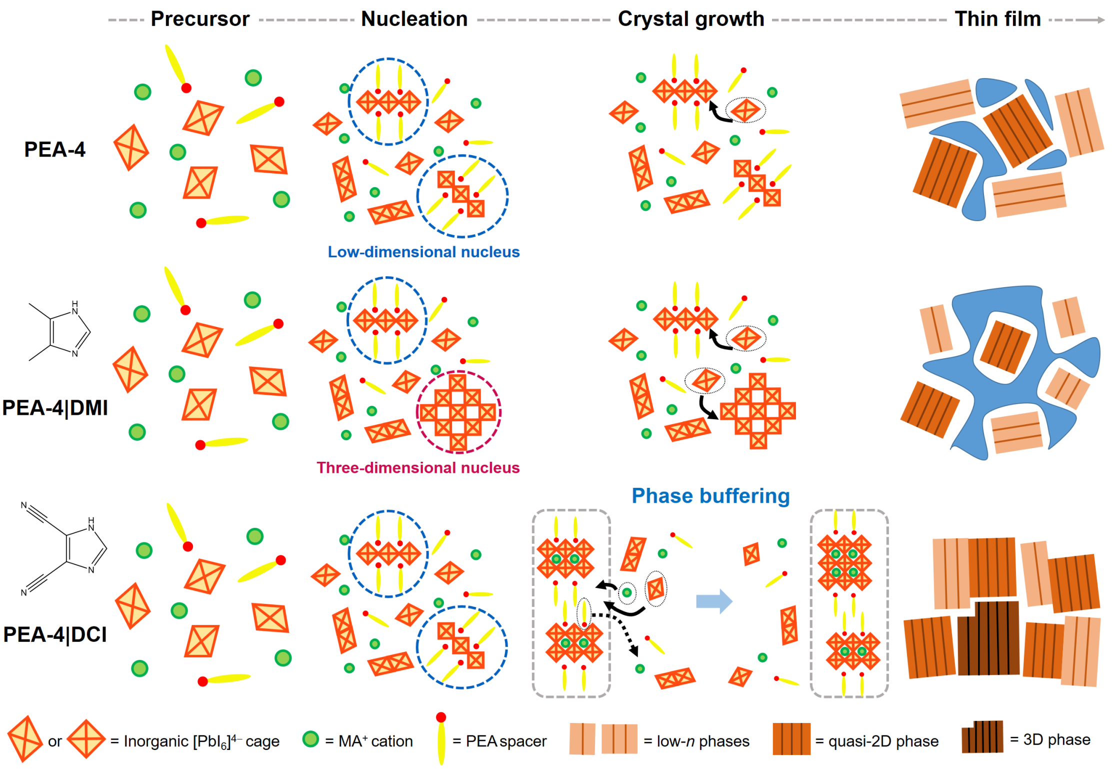

Scheme S1. Schematic of crystallization process in neat and DMI / DCI-treated PEA-4 samples.

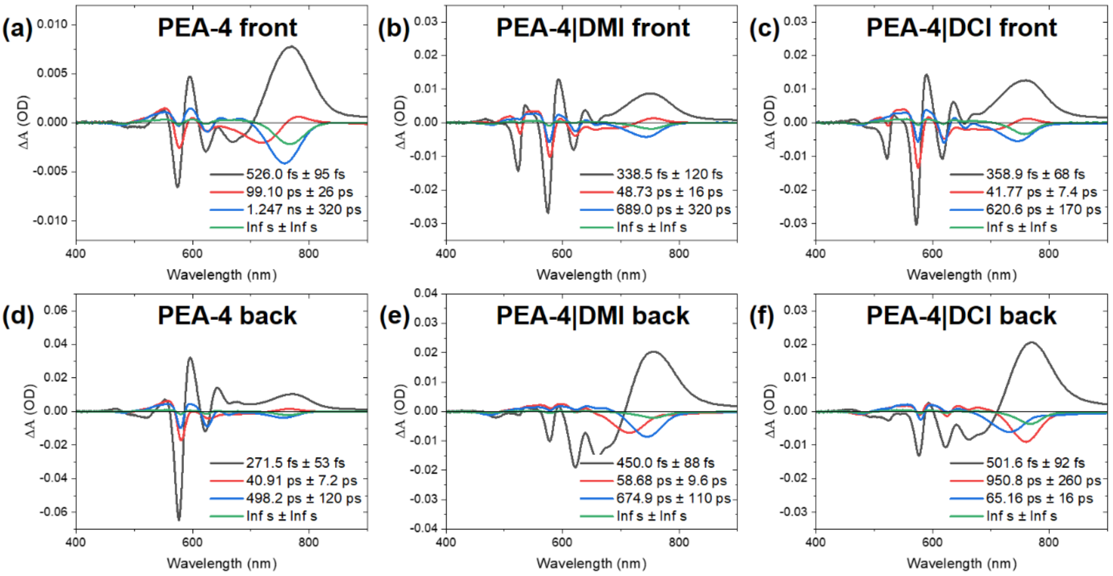

Fig. S12 SVD fitting results of neat and DMI / DCI-treated PEA-4 perovskites upon photo-excitation from front side (a–c) and back side (d–f), respectively.

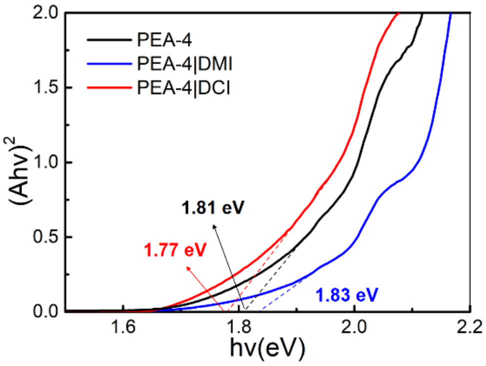

Fig. S13 Tauc plots of neat and additive-treated PEA-4 2D perovskites.

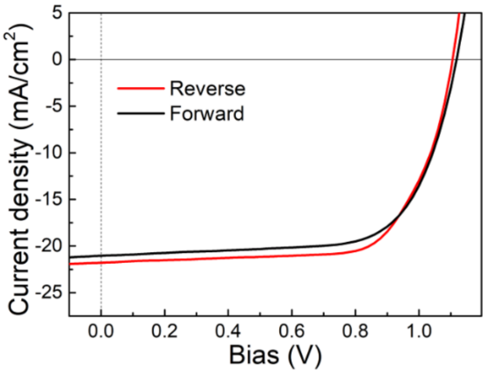

Fig. S14. Photo-*J*–*V* curves of DCI-treated PEA-4 based solar cell with reverse and forward scan directions under AM1.5G simulated light irradiation.

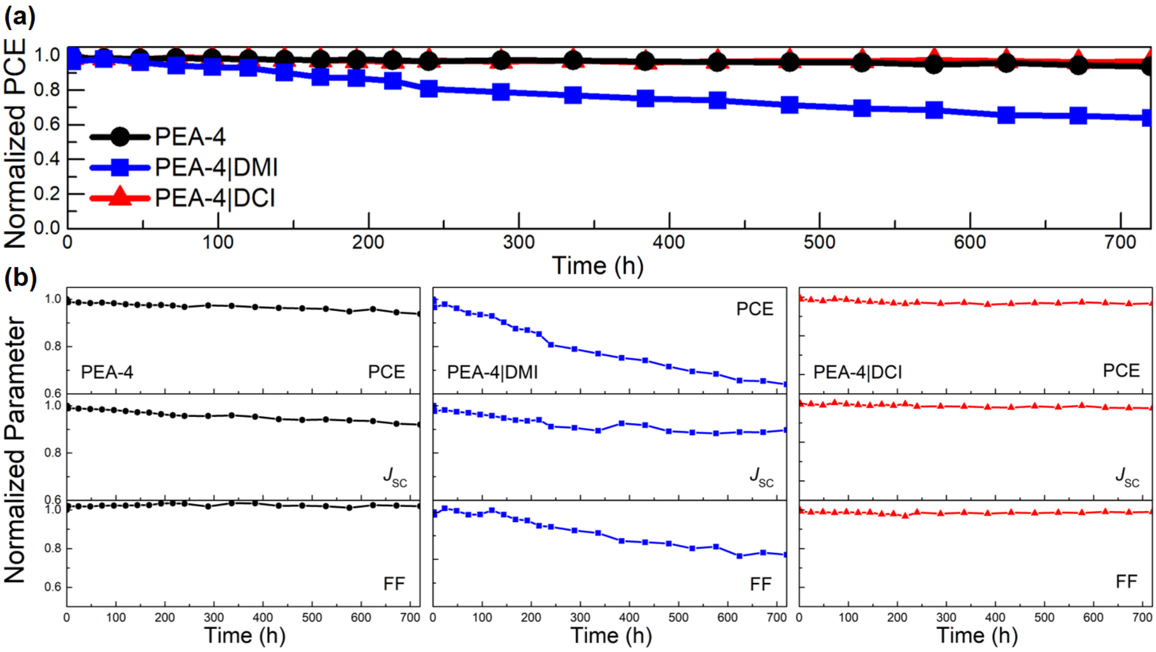

Fig. S15. (a) Normalized PCE and (b) corresponding parameters of neat, DMI and DCI-treated PEA-4 based solar cells stored in N_2 filled glovebox over 700 h.

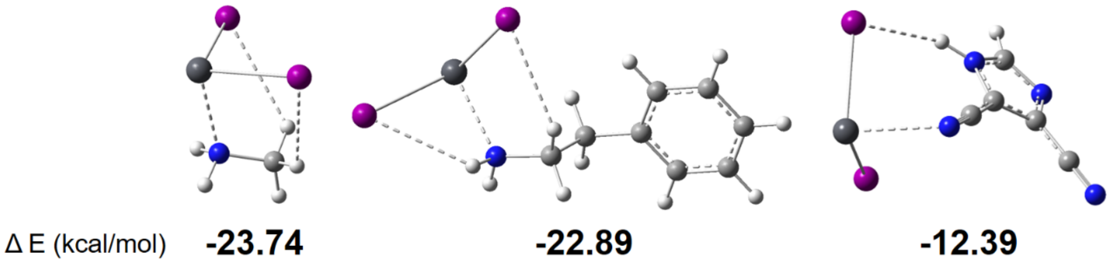

Fig. S16 The intermolecular binding energy values as calculated by Gaussian between PbI_2 and MA, PEA and DCI, respectively.

Table S2. Summary of photovoltaic parameters of the state-of-the art 2D RPPs ($n \leqslant 4$) based planar solar cells

Sample	*n* value	J_{SC} (mA/cm^2)	V_{OC} (V)	FF (%)	PCE (%)
$(3AMP)(MA_{0.75}FA_{0.25})_3Pb_4I_{13}$	4	19.51	1.24	77.27	18.67[S1]
$PEA_2MA_3Pb_4I_{13}$	4	18.52	1.20	83.39	18.48[S2]
$F\text{-}PEA_2MA_3Pb_4I_{13}$	4	19.04	1.21	78.5	18.10[S3]
$(BM)(BA)MA_3Pb_4I_{13}$	4	19.8	1.15	76.3	17.3[S4]
$BA_2MA_3Pb_4I_{13}$	4	17.56	1.20	81.1	17.1[S5]
$PEA_2MA_3Pb_4I_{13}$	4	18.47	1.17	79.13	17.03[S6]
$ThFA_2MA_2Pb_3I_{10}$	3	20.17	1.05	79.0	16.72[S7]
$BA_2MA_3Pb_4I_{13}$	4	18.67	1.18	74.80	16.48[S8]
$(BA)_{1.6}(MA)_{3.4}Pb_4I_{13}$	4	20.44	1.07	74.45	16.29[S9]
$BA_2MA_3Pb_4I_{13}$	4	16.75	1.31	74.07	16.25[S10]
$(PBA_{0.5}BA_{0.5})_2MA_3Pb_4I_{13}$	4	17.3	1.19	78.0	16.0[S11]
$PEA_{0.2}BA_{1.8}MA_3Pb_4I_{13}$	4	16.51	1.29	74	15.81[S12]
$Gly\text{-}(Cs_{0.05}FA_{0.95}\text{-}PbI_3)_{0.9}(FAPbBr_3)_{0.1}$	4	20.86	1.05	70.98	15.61[S13]
$(BA_{0.9}PEA_{0.1})_2MA_3Pb_4I_{13}$	4	17.12	1.182	76.40	15.46[S14]
$FPEA_2MA_3Pb_4I_{13}$	4	13.7	1.08	74	15.2[S15]
$(PPA)_2(Cs_{0.05}(FA_{0.88}MA_{0.12})_{0.95})_3$	4	19.33	1.14	67	14.76[S16]

$-Pb_4(I_{0.88}Br_{0.12})_{13}$					
$BDA_2MA_3Pb_4I_{13}$	4	19.9	1.12	64.2	14.38[S17]
$(PDA)FA_3Pb_4I_{13}$	4	17.30	1.10	72.5	13.8[S18]
$BA_2MA_3Pb_4I_{13}$	4	14.2	1.10	71	11.1[S19]

Table S3. Comparative summary of −SCN unit and S atom exploited in 2D halide perovskites in literature

	Molecule	**Role**	**Reference**
S atom	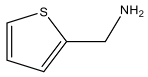	Spacer	[S20, S21]
	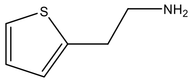	Spacer	[S22]
	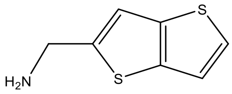	Spacer	[S23]
	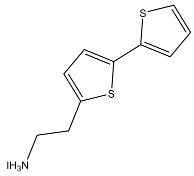	Spacer	[S24]
	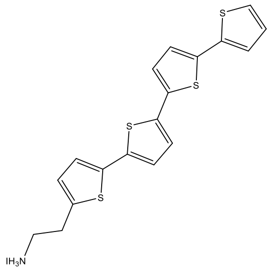	Spacer	[S24]
	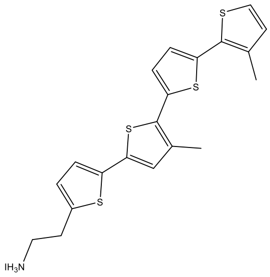	Spacer	[S24, S25]

	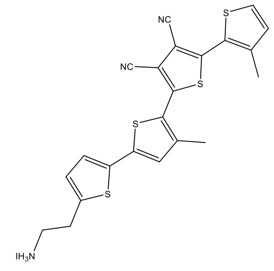	Spacer	[S24]
	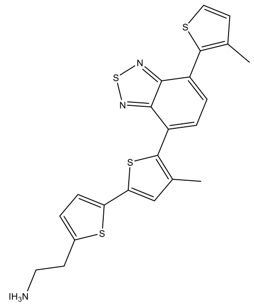	Spacer	[S24]
	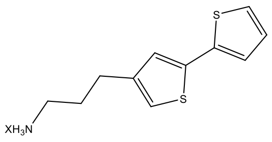	Spacer	[S26]
	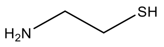	Spacer	[S27]
	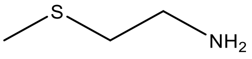	Spacer	[S28]
–SCN unit	$Pb(SCN)_2$	Additive	[S29]
	NH_4SCN	Additive	[S30-S33]
	MASCN	Additive	[S34]
	$(CH_3NH_3)_2Pb(SCN)_2I_2$	Precursor	[S35]
	$CH_3NH_3Pb(SCN)_2I$	Precursor	[S36]
	CuSCN	Interface	[S37]

Reference:

[S1] H. Wu, X. Lian, J. Li, Y. Z. Zhang, G. Zhou, X. Wen, Z. Xie, H. Zhu, G. Wu and H. Chen, *J. Mater. Chem. A* 2021, **9**, 12566.

[S2] Y. Yang, C. Liu, O. A. Syzgantseva, M. A. Syzgantseva, S. Ma, Y. Ding, M. Cai, X. Liu, S. Dai and M. K. Nazeeruddin, *Adv. Energy Mater*. 2021, **11**, 2002966.

[S3] Z. Wang, Q. Wei, X. Liu, L. Liu, X. Tang, J. Guo, S. Ren, G. Xing, D. Zhao and Y. Zheng, *Adv. Funct. Mater*. 2021, **31**, 2008404.

[S4] C. Liu, Z. Fang, J. Sun, Q. Lou, J. Ge, X. Chen, E. Zhou, M. Shang, W. Yang and Z. Ge, *ACS Energy Lett*. 2020, **5**, 3617−3627.

[S5] S. Sidhik, W. Li, M. H. K. Samani, H. Zhang, Y. Wang, J. Hoffman, A. K. Fehr, M. S. Wong, C. Katan, J. Even, A. B. Marciel, M. G. Kanatzidis, J. C. Blancon and A. D. Mohite, *Adv. Mater.* 2021, **33**, 2007176.

[S6] Y. Yang, C. Liu, A. Mahata, M. Li, C. Roldan-Carmona, Y. Ding, Z. Arain, W. Xu, Y. Yang, P. A. Schouwink, A. Zuttel, F. De Angelis, S. Dai and M. K. Nazeeruddin, *Energy Environ. Sci*. 2020, **13**, 3093.

[S7] Y. Dong, D. Lu, Z. Xu, H. Lai and Y. Liu, *Adv. Energy Mater*. **2020**, 10, 2000694.

[S8] J. Song, G. Zhou, W. Chen, Q. Zhang, J. Ali, Q. Hu, J. Wang, C. Wang, W. Feng, A. B. Djurisic, H. Zhu, Y. Zhang, T. Russell and F. Liu, *Adv. Mater.* 2020, **32**, 2002784.

[S9] X. Li, G. Wu, J. Zhou, J. Zhang, X. Zhang, B. Wang, H. Xia, H. Zhou and Y. Zhang, *Small* 2020, **16**, 1906997.

[S10] C. Liang, H. Gu, Y. Xia, Z. Wang, X. Liu, J. Xia, S. Zuo, Y. Hu, X. Gao, W. Hui, L. Chao, T. Niu, M. Fang, H. Lu, H. Dong, H. Yu, S. Chen, X. Ran, L. Song, B. Li, J. Zhang, Y. Peng, G. Shao, J. Wang, Y. Chen, G. Xing and W. Huang, *Nat. Energy* 2021, **6**, 38.

[S11] S. Chen, N. Shen, L. Zhang, L. Zhang, S. H. Cheung, S. Chen, S. K. So and B. Xu, *Adv. Funct. Mater*. 2020, **30**, 1907759.

[S12] X. Lian, L. Zuo, H. Wu, G. Zhou, C. Lin, H. Zhu, G. Wu, D. Cahen and H. Chen, *J. Mater. Chem. A* 2020, **8**, 22175.

[S13] H. Zheng, W. Wu, H. Xu, F. Zheng, G. Liu, X. Pan and Q. Chen, *Adv. Funct. Mater*. 2020, **30**, 2000034.

[S14] N. Zhou, B. Huang, M. Sun, Y. Zhang, L. Li, Y. Lun, X. Wang, J. Hong, Q. Chen and H. Zhou, *Adv. Energy Mater*. 2020, **10**, 1901566.

[S15] J. Liang, Z. Zhang, Y. Zheng, X. Wu, J. Wang, Z. Zhou, Y. Yang, Y. Huang, Z. Chen and C. Chen, *J. Mater. Chem. A* 2021, **9**, 11741.

[S16] J. Xi, I. Spanopoulos, K. Bang, J. Xu, H. Dong, Y. G. Yang, C. D. Malliakas, J. M. Hoffman, M. G. Kanatzidis and Z. Wu, *J. Am. Chem. Soc.* 2020, **142**, 19705−19714.

[S17] Y. Zhang, J. Wen, Z. Xu, D. Liu, T. Yang, T. Niu, T. Luo, J. Lu, J. Fang, X. Chang, S. Jin, K. Zhao and S. Liu, *Adv. Sci*. 2021, **8**, 2001433.

[S18] L. Cheng, Z. Liu, S. Li, Y. Zhai, X. Wang, Z. Qiao, Q. Xu, K. Meng, Z. Zhu and G. Chen, *Angew. Chem. Int. Ed.* 2021, **60**, 856.

[S19] A. Caiazzo, K. Datta, J. Jiang, M. C. Gelvez-Rueda, J. Li, R. Ollearo, J. M. Vicent-Luna, S. Tao, F. C. Grozema, M. M. Wienk and R. A. J. Janssen, *Adv. Energy Mater*. 2021, **11**, 2102144.

[S20] Z. Jiang, Y. Hao, H. Wang, X. Zhang, J. Yao, M. Li and Z. Wei, *J. Solid State Chem*. 2020, **282**, 121104.

[S21] H. Lai, B. Kan, T. Liu, N. Zheng, Z. Xie, T. Zhou, X. Wan, X. Zhang, Y. Liu and Y. Chen, *J. Am. Chem. Soc.* 2018, **140**, 11639–11646.

[S22] Y. Yan, S. Yu, A. Honarfar, T. Pullerits, K. Zheng and Z. Liang, *Adv Sci*. 2019, **6**, 1900548.

[S23] H. Hu, F. Meier, D. Zhao, Y. Abe, Y. Gao, B. Chen, T. Salim, E. E. M. Chia, X. Qiao, C. Deibel and Y. Lam, *Adv. Mater*. 2018, **30**, 1707621.

[S24] Y. Gao, E. Shi, S. Deng, S. B. Shiring, J. M. Snaider, C. Liang, B. Yuan, R. Song, S. M. Janke, A. Liebman-Pelaez, P. Yoo, M. Zeller, B. W. Boudouris, P. Liao, C. Zhu, V. Blum, Y. Yu, B. M. Savoie, L. Huang and L. Dou, *Nat. Chem*. 2019, **11**, 1151–1157.

[S25] K. Ma, H. R. Atapattu, Q. C. Zhao, Y. Gao, B. P. Finkenauer, K. Wang, K. Chen, S. M. Park, A. H. Coffey, C. Zhu, L. Huang, K. R. Graham, J. G. Mei and L. T. Dou, *Adv. Mater*. 2021, **33**, 2100791.

[S26] P. H. Denis, M. Mertens, W. T. M. Van Gompel, K. Van Hecke, B. Ruttens, J. D'Haen, L. Lutsen and D. Vanderzande, *Chem. Mater*. 2021, **33**, 5177−5188.

[S27] P. Kour, M. C. Reddy, S. Pal, S. Sidhik, T. Das, P. Pandey, S. P. Mukherjee, S. Chakraborty, A. D. Mohite and S. Ogale, *Angew. Chem. Int. Ed.* 2021, **60**, 18750–18760.

[S28] H. Ren, S. Yu, L. Chao, Y. Xia, Y. Sun, S. Zuo, F. Li, T. Niu, Y. Yang, H. Ju, B. Li, H. Du, X. Gao, J. Zhang, J. Wang, L. Zhang, Y. Chen and W. Huang, *Nat. Photon*. 2020, **14**, 154−163.

[S29] Y. Sun, J. Peng, Y. Chen, Y. Yao and Z. Liang, *Sci. Rep.* 2017, **7**, 46193.

[S30] W. Fu, J. Wang, L. Zuo, K. Gao, F. Liu, D. S. Ginger and A. K. Y. Jen, *ACS Energy Lett.* 2018, **3**, 2086−2093.

[S31] X. Zhang, G. Wu, W. Fu, M. Qin, W. Yang, J. Yan, Z. Zhang, X. Lu and H. Chen, *Adv. Energy Mater*. 2018, **8**, 1702498.

[S32] X. Zhang, G. Wu, S. Yang, W. Fu, Z. Zhang, C. Chen, W. Liu, J. Yan, W. Yang and H. Chen, *Small* 2017, **13**, 1700611.

[S33] Y. Zhang, J. Chen, X. Lian, W. Yang, J. Li, S. Tian, G. Wu and H. Chen, *Sci China Chem*. 2019, **62**, 859.

[S34] F. Li, J. Zhang, S. Jo, M. Qin, Z. Li, T. Liu, X. Lu, Z. Zhu and A. K. Y. Jen, *Small Methods* 2020, **4**, 1900831.

[S35] A. M. Ganose, C. N. Savory, D. O. Scanlon, *J. Mater. Chem. A* 2017, **5**, 7845–7853.

[S36] Q. Jiang, D. Rebollar, J. Gong, E. L. Piacentino, C. Zheng and T. Xu, *Angew. Chem. Int. Ed.* 2015, **54**, 7617–7620.

[S37] J. Chen, J. Y. Seo and N. G. Park, *Adv. Energy Mater*. 2018, **8**, 1702714.